ELSEVIER

Nuclear Physics B (Proc. Suppl.) 54B (1997) 167–175

NUCLEAR PHYSICS B
PROCEEDINGS
SUPPLEMENTS

The VIRGO Interferometer For Gravitational Wave Detection

B. Caron, A. Dominjon, C. Drezen, R. Flaminio, X. Grave, F. Marion, L. Massonnet, C. Mehmel, R. Morand, B. Mours, V. Sannibale, M. Yvert
Laboratoire de Physique des Particules (LAPP), IN2P3-CNRS, 74941 Annecy-Le-Vieux Cedex, France

D. Babusci, S. Bellucci, S. Candusso, G. Giordano, G. Matone
Laboratori Nazionali dell'INFN (LNF-INFN), 00044 Frascati, Italy

J.-M. Mackowski, L. Pinard
Université Claude Bernard, IPNL, IN2P3-CNRS, 69622 Villeurbanne Cedex, France

F. Barone, E. Calloni, L. Di Fiore, M. Flagiello, F. Garuti, A. Grado, M. Longo, M. Lops, S. Marano, L. Milano, S. Solimeno
Dipartimento di Scienze Fisiche dell'Università e INFN Sezione di Napoli, 80125 Napoli, Italy

V. Brisson, F. Cavalier, M. Davier, P. Hello, P. Heusse, P. Mann
Laboratoire de l'Accélérateur Linéaire, Université Paris-Sud, IN2P3-CNRS, 91405 Orsay CEDEX, France

Y. Acker*, M. Barsuglia, B. Bhawal, F. Bondu, A. Brillet, H. Heitmann, J.-M. Innocent, L. Latrach, C. N. Man, M. Pham-Tu, E. Tournier, M. Taubmann, J.-Y. Vinet
Laser Optique Orsay, Université Paris-Sud, IN2P3-CNRS, 91405 Orsay CEDEX, France

C. Boccara, Ph. Gleyzes, V. Loriette, J.-P. Roger
Laboratoire de Spectroscopie en Lumière Polarisée, Ecole Supérieure de Physique et Chimie Industrielle, 75005 Paris, France

G. Cagnoli, L. Gammaitoni, J. Kovalik, F. Marchesoni, M. Punturo
Dipartimento di Fisica dell'Università e INFN Sezione di Perugia, 06100 Perugia, Italy

M. Beccaria, M. Bernardini, E. Bougleux†, S. Braccini, C. Bradaschia, G. Cella, A. Ciampa, E. Cuoco, G. Curci, R. Del Fabbro, R. De Salvo, A. Di Virgilio, D. Enard‡, I. Ferrante, F. Fidecaro§, A. Giassi, A. Giazotto, L. Holloway¶, P. La Penna, G. Losurdo, S. Mancini, M. Mazzoni†, F. Palla, H.-B. Pan, D. Passuello, P. Pelfer†, R. Poggiani, R. Stanga†, A. Vicere', Z. Zhang
Dipartimento di Fisica dell'Università, INFN Sezione di Pisa e Scuola Normale Superiore, 56010 S. Piero a Grado, Italy

V. Ferrari, E. Majorana, P. Puppo, P. Rapagnani, F. Ricci
Dipartimento di Fisica dell'Università "La Sapienza" e INFN Sezione di Roma 1, 00185 Roma, Italy

The Virgo gravitational wave detector is an interferometer with 3 km long arms in construction near Pisa in Italy. The accessible sources at the design sensitivity and main noises are reviewed. Virgo has devoted a significant effort to extend sensitivity to low frequency reaching the strain level $\tilde{h} = 10^{-21}\,\mathrm{Hz}^{-1/2}$ at 10 Hz while at 200 Hz $\tilde{h} = 3 \cdot 10^{-23}\,\mathrm{Hz}^{-1/2}$. Design choices and status of construction are presented.

1. INTRODUCTION

Observation of light deviation by the Sun in 1919[1] was a spectacular confirmation of the predictions of General Relativity Theory. This theory had also been able to interpret in a natural way the precession of Mercury orbit perihelion. Still the measurements were at the 10% level (ex-

*INSU-CNRS, France.
†INFN Firenze, Italy.
‡On leave from ESO, Garching, Germany.
§To whom correspondence should be addressed.
¶University of Illinois, Urbana-Champaigne, USA.

PII: S0920-5632(97)00109-6

cept Eötvös-like experiments) and it was necessary to wait until the '60s to perform other, more precise checks of the theory. These were possible by timing the radar echo from planets of the solar system first, and from artificial satellites[2] then. Mössbauer effect allowed also observation on Earth of a gravitational red shift[3], another prediction related to General Relativity. Currently these and other measurements put rather stringent limits on alternative theories that could challenge General Relativity.

Still these measurements have been performed in static conditions, namely with a gravitational field constant in time. A most interesting prediction of the theory in non static conditions is the emission of gravitational waves by accelerated masses.

If one considers a small perturbation the Einstein equations can be linearized and turn out to have propagating solutions[4]. Indirect demonstration of the existence of gravitational waves was obtained by Taylor and Hulse[5] through the study of the orbit of a binary neutron star system. Today these neutron star systems together with the static measurements show that General Relativity is in agreement with experiment at a fraction of percent[6].

The direct detection of gravitational waves would allow to measure quantities inaccessible to astronomical observations, like the tensor nature of the wave, or the modalities of emission if a model for the source is available. Moreover a new field can open if sensitivity becomes sufficient to reach detection rates of tens or hundreds of events per year: gravitational wave astronomy may start providing independent information on the Universe, complementing the knowledge accumulated in centuries of electromagnetic observation.

This programme is a formidable challenge to experimentalists as gravitational waves induce inconceivable tiny motion of matter; first efforts for direct detections were performed using resonating bars, sensitive only in a small interval around the resonance frequency. Wide band detectors based on interferometry have been developed and some large ones are now in construction in various places.

In this article, after reviewing properties of gravitational radiation we discuss the properties of the sources that could be detected and the noises that currently limit sensitivity. The Virgo interferometer components are described together with the status of construction.

2. Gravitational radiation

General relativity postulates that space-time is in general curved and that curvature is caused by the presence of mass. In flat space the infinitesimal interval ds^2 is determined by the symmetric tensor $\eta_{\mu\nu}$ defined by

$$ds^2 = dt^2 - dx^2 - dy^2 - dz^2 = dx^\mu dx^\nu \eta_{\mu\nu} \quad (1)$$

(c=1). A small perturbation to flat space is described by the dimensionless tensor $h_{\mu\nu}$

$$ds^2 = dx^\mu dx^\nu (\eta_{\mu\nu} + h_{\mu\nu}). \quad (2)$$

For a propagating wave along the z direction $h_{\mu\nu}$ can be cast in the form of an oscillating scalar times

$$\begin{pmatrix} 0 & 0 & 0 & 0 \\ 0 & h_+ & h_\times & 0 \\ 0 & h_\times & -h_+ & 0 \\ 0 & 0 & 0 & 0 \end{pmatrix} \quad (3)$$

if the "transverse traceless" (TT) coordinate gauge is chosen. Only two independent amplitudes, h_+ and $h_\times$ describe the wave, corresponding to two polarization states.

In this gauge two free-falling mirrors remain at distance L along the x direction but the light round trip time becomes

$$t_1 - t_0 = \frac{2L}{c}\left[1 - \frac{h_+(t_0)}{2}\frac{\sin\frac{\Omega_g L}{c}}{\frac{\Omega_g L}{c}}\right] \quad (4)$$

when a wave of angular frequency Ω_g travels along the z direction.

In a different gauge one observes equivalently that the distance between mirrors changes by

$$\delta x = \frac{h(t_0)}{2} L \frac{\sin\frac{\Omega_g L}{c}}{\frac{\Omega_g L}{c}}. \quad (5)$$

Position noise must be of the order of $5 \cdot 10^{-20}$ m.

3. Sources accessible to ground based detectors

Likely astrophysical sources of gravitational radiation can be classified according to the emission duration[7]. Bursts caused by stellar collapse last only milliseconds; inspiralling of tight binary stars can be observed instead over a time ranging from a few seconds to several hours. With a sensitivity for the strain h around 10^{-23}, events located in the Virgo cluster can be detected with a rate of a few events per year. As a matter of fact today's estimates for these rates span two orders of magnitude.

Rotating systems with low dissipation like spinning neutron stars or loose binary star systems emit over much longer times single frequency waves. In the case of neutron stars the amplitude appears to be too low to be detected by currently planned interferometers, unless suitable averaging of noise is performed.

Stochastic background is predicted to be always present with a continuous frequency spectrum extending, according to classical big bang model up to a few tens of kHz but with amplitude out of reach of the present detectors. Recent work on superstrings[8] resumed interest for this source by suggesting that the spectrum could extend up to 10^6–10^9 Hz, a region where no astrophysical contribution is expected.

3.1. Coalescence observation

Inspiralling binary neutron stars show an increase in radiation frequency ν given by

$$\nu(t) \propto (t_0 - t)^{-3/8} \tag{6}$$

where t_0 is the time coalescence occurs, neglecting higher order corrections. The amplitude h is related to the wave frequency by

$$h(\nu) \propto \nu^{2/3}. \tag{7}$$

The signal-to-noise ratio (SNR) in each frequency bin is given by the ratio between $\tilde{h}(\nu)$ and the noise $\tilde{n}(\nu)$ averaged quadratically over the time $\mathrm{d}t/\mathrm{d}\nu$ spent in a 1 Hz bin

$$\frac{\mathrm{dSNR}^2}{\mathrm{d}\nu} \propto \tilde{h}(\nu)^2 \frac{\mathrm{d}t/\mathrm{d}\nu}{\tilde{n}(\nu)^2} \propto \frac{\nu^{-7/3}}{\tilde{n}(\nu)^2}. \tag{8}$$

Contributions at different frequencies must be summed quadratically and SNR will be higher the more the integral can be extended on the low frequency side. In addition, if the detection band starts, say, at 100 Hz only the last couple of seconds of life of the binary system can be followed. By being sensitive from 10 Hz onwards such a signal could last in the detector for more than one thousand seconds, allowing for additional consistency checks on event candidates.

3.2. Low frequency sensitivity and neutron stars

Rapidly rotating neutron stars are also candidates for emitting gravitational radiation. The expected amplitude is given by

$$h \sim 4 \cdot 10^{-25} \left(\frac{1\,\mathrm{ms}}{T}\right)^2 \left(\frac{1\,\mathrm{kpc}}{r}\right) \times \tag{9}$$

$$\left(\frac{I}{10^{38}\,\mathrm{kg\,m^2}}\right) \left(\frac{\epsilon}{10^{-7}}\right) \tag{10}$$

where T is the rotation period, r the distance, I the moment of inertia and ϵ the ellipticity. No precise estimate of ϵ is available; upper limits are given by attributing to gravitational radiation the observed decrease in rotation speed. The amplitude of the emitted waves is such that only neutron stars in our Galaxy have some probability of being detected.

The frequency spectrum of a sample of the known pulsars[9] is shown in figure 1. The emission frequency peaks around a few Hz and a substantial tail of observations extends to higher frequencies (millisecond pulsars). No firm conclusions can be drawn on the parent star population from the observed pulsars. However considering the estimated number of neutron stars in our Galaxy (of the order of 10^9), the pulsar frequency distribution justifies the effort of extending sensitivity to the few Hz region.

4. Detection of a gravitational wave signal

The simplest detection procedure would consist in accepting only signals above a certain threshold. This is a non optimal approach because it does not take into the detector noise and the properties of the signal (when these are

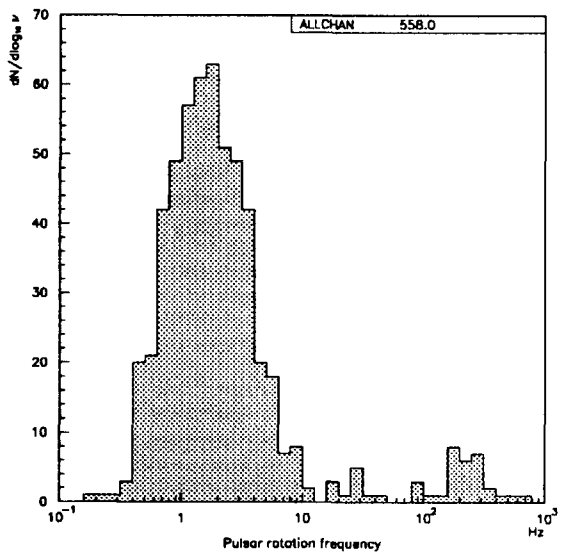

Figure 1. Distribution of the pulsar rotation frequency. The quadrupole gravitational radiation has double frequency.

known). The incoming signal can indeed be filtered by attenuating unwanted frequency components. When the signal shape is known (as could be the case for coalescing binaries) optimal performance is achieved by *Wiener filtering*. This can be seen as an attenuation of the detector output at frequencies where noise is high or signal is low and an enhancement at frequencies where the signal is high or the detector is more quiet.

Let $S_n(\nu)$ the noise power spectrum ($\sqrt{S_n(\nu)}$ is the r.m.s. amplitude in a 1 Hz bin) and $\tilde{h}(\nu)$ the Fourier transform of the expected signal of an event at time $t = 0$ then the Wiener filtered signal s_W is given by

$$s_W = \int_{-\infty}^{+\infty} \frac{\tilde{s}(\nu)\tilde{h}^*(\nu)}{S_n(\nu)}\,\mathrm{d}\nu \qquad (11)$$

that is the Fourier transform $\tilde{s}(\nu)$ of the detector signal $s(t)$ is weighted by

$$\frac{\tilde{h}^*(\nu)}{S_n(\nu)}.$$

For a white spectrum ($S_n(\nu) = 1$) this becomes in the time domain

$$s_W = \int_{-\infty}^{+\infty} s(t)h^*(-t)\,\mathrm{d}t \qquad (12)$$

with $h^*(-t) = h(t)$ (also known as *matched filter*.) These analyses will be performed for all possible event times using digital filters, giving $s_W(t)$.

A threshold can now be set on the quantity $s_W(t)$ to decide whether and when an event from a well defined source, has occurred.

This filter can be used to discriminate between different sources by comparing the $s_W(t)$ computed under different hypotheses and selecting the one with the highest s_W. Discrimination is more efficient if the $\tilde{h}(\nu)$ differ significantly for the various sources; this is more likely to happen if there is a wide frequency band. These considerations point at the importance of having the widest possible band for the detector, not only because more sources become accessible, but also for the capability of identifying them reliably.

5. The Virgo wide band detector

The Virgo interferometer measures the distance between essentially free masses at 3 km one from the other. The design noise level is $\tilde{h} \sim 10^{-21}/\sqrt{\text{Hz}}$ at 10 Hz and $\tilde{h} \sim 3 \cdot 10^{-23}/\sqrt{\text{Hz}}$ at 200 Hz. The design sensitivity extends from 4-5 Hz to 6 kHz.

The noise in such a detector comes first of all from the residual motion of the masses involved. As order of magnitude current wide band detectors aim at a position noise of the order of $10^{-19}\,\text{m}/\sqrt{\text{Hz}}$ at 100 Hz. Ground motion is many orders of magnitude larger and has to be filtered. Position noise due to thermal fluctuations is the next limitation and is the target of many R&D programs. A fundamental limit for Earth based detectors is local gravity fluctuations around the detection masses.

The expected displacements can be detected by interferometric distance measurements. It is necessary to increase the light path through multiple reflections and in Virgo Fabry-Pérot cavities are used. Noise in such a measurement comes firstly

from variations in light wavelength. This can be dealt with by stabilizing the light source and measuring two lengths simultaneously. By performing measurements in perpendicular directions one takes advantage of the nature of the gravitational wave: in particular for arms along x and y directions and a wave propagating along z one round trip time will increase and the other decrease by the same amount doubling the signal. In the general case the detector response will depend on the direction and polarization of the wave.

Another limitation comes from photon counting in the interference pattern. The shot noise introduced can however be reduced by increasing light intensity. In addition to the increase in source power it is possible to recirculate the light beam not used in the measurement process. Finally, at a level not relevant today the Heisenberg principle puts a fundamental limitation (though studies are going on to go around $\Delta\phi\Delta N > 2\pi$).

Elaboration of these concepts has resulted in an apparatus where the elements of a complex interferometer, carefully suspended to seismic attenuators, play the role of detection masses.

6. The proof mass suspensions

6.1. Seismic Isolation

The observed spectrum on the Virgo site in the 1 Hz region is roughly described by

$$\tilde{x}(\nu) = 10^{-6}/\nu^2\,\mathrm{m}/\sqrt{\mathrm{Hz}} \qquad (13)$$

when ν is expressed in Hz. For a 3 km interferometer an attenuation of at least 10^{10} must be achieved to detect strains $\tilde{h} \sim 10^{-23}/\sqrt{\mathrm{Hz}}$ from a few Hz onwards.

When one extremity of a spring with a mass at the other end moves, the amplitude of motion of the mass has the well known textbook resonant behaviour as function of the driving frequency ν. Calling ν_0 the resonance frequency, motion decreases as ν_0^2/ν^2 when $\nu \gg \nu_0$. Following this principle seismic noise filtering is obtained by suspending the detection masses to a cascade of harmonic oscillators. Simplicity of behaviour is obtained by using a pendulum as harmonic oscillator, with gravity as loss free spring. For N identical harmonic oscillators an attenuation

$$A \propto (\frac{\nu_0}{\nu})^{2N} \qquad (14)$$

is obtained for frequencies well above the normal mode frequencies of the system. When it comes out to build such a system practical sizes set ν_0 between 100 mHz and 1 Hz.

Oscillations at the normal mode frequencies may have such an amplitude to take the detector away from its working point. Damping of these modes must be performed without introducing additional noise by acting at the top of the chain, before seismic filters. The active control loop is based on position measurements with respect to ground and on accelerometers, constructed by Firenze. These allow to reduce the motion of the suspension point so that chain modes will not be excited.

A further stage called marionetta, built by Roma, holds and steers the mirror by means of four wires forming thus another pendulum stage 70 cm long. The marionetta supports a reference mass that allows to apply a force on the mirror from a quiet support. Figure 2 shows schematically the suspension together with the seven filters, the marionetta and the mirror. The whole system is kept in vacuum inside a stainless steel tower.

The present design results in an attenuation from suspension point to the mirror of $\sim 10^{-10}$ at 4 Hz setting the low frequency limit for the VIRGO sensitivity well below 10 Hz.

6.2. Compensation of tides and long term motion

Ground motion can be of the order of hundreds of micron due to tidal deformation of the Earth crust and to thermal effects on surface. Such effects have frequencies outside the detection band of Virgo but need to be compensated to meet the stringent requirements on the interferometer working point (for the Fabry-Pérot mirrors the r.m.s. fluctuation must be reduced to $6 \cdot 10^{-6}\lambda$.) The required dynamic range is 10^{14} above the noise floor, well above what a single device can achieve.

Control of the mirror position is achieved in three different places. The fine control that

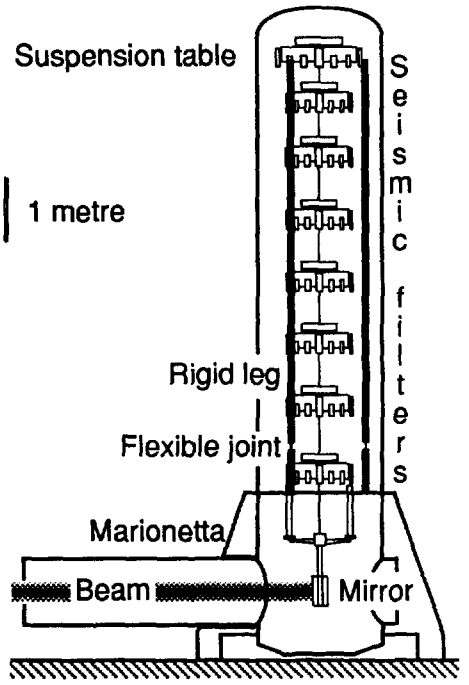

Figure 2. The VIRGO mirror suspension.

should not introduce any noise is performed from a reference mass suspended to the marionetta. A rougher control is applied on the marionetta itself, relying on the filtering characteristics of the last pendulum. Finally by moving the suspension point the necessary dynamic range is achieved.

The solution adopted for moving the whole suspension (1.2 ton) is to have a support structure that can be deformed. A three-leg system with flexible joints at feet supports the suspension point. The low resonant frequency of this inverted pendulum gives an additional attenuation and the noise introduced when motion is required comes only from internal friction of the joints. Rolling or sliding systems, which must be greased and give problems when a clean vacuum is needed, are thus eliminated.

6.3. Thermal noise

The detection masses are in thermal equilibrium with the environment. An average energy of kT is associated with each oscillation degree of freedom, resulting in position fluctuations for the macroscopic coordinates too. The frequency spectrum is determined by the dissipation mechanism associated with that motion and can be computed using the fluctuation-dissipation theorem [10] starting from the equation of motion.

Internal friction in materials can be described by adding[11] to the elastic constant of an harmonic oscillator an imaginary term so that the equation of motion reads

$$m\ddot{x} + k(1 + i\phi)x = 0 \qquad (15)$$

Values for ϕ of 10^{-3}, essentially constant over the range of frequency of interest, have been measured in harmonic steel wires.

The noise spectrum is

$$\tilde{x}(\omega) = \sqrt{\frac{4kT\omega_0}{mQ}} \frac{1}{\sqrt{(\omega_0^2 - \omega^2)^2 + \omega^2\omega_0^2/Q^2}}$$

for viscous damping while for internal friction one has

$$\tilde{x}(\omega) = \sqrt{\frac{4kT\phi\omega_0}{m}} \sqrt{\frac{\omega_0}{\omega}} \frac{1}{\sqrt{(\omega_0^2 - \omega^2)^2 + \phi^2\omega_0^4}}$$

resulting in a different dependence on ω (at resonance $Q = \phi^{-1}$. For $\omega^2 \gg k/m$ the spectrum behaves like $\omega^{-5/2}$ while for $\omega^2 \ll k/m$ a $\omega^{-1/2}$ dependence is obtained.

Virgo assumes that dissipation of the mirror pendulum can be limited to internal friction, while gravity does not dissipate, allowing to reach a Q of 10^6. Recent measurements in Perugia have reached this target. Similarly measurements in Orsay have achieved $Q = 10^6$ for mirrors too.

7. The distance measurement

The detection is based on the comparison of the phases of light coming from two Fabry-Pérot cavities. This is achieved optically by letting the beams interfere and detecting light intensity variations.

The detailed optical scheme of Virgo is shown in figure 3. Light is produced by a 20 W Nd-YAG laser stabilized in frequency by means of reference cavity made out of ultra low expansion material (ULE[13]). To keep only the TEM_{00} mode

a filtering cavity (mode cleaner) is used. A beam splitter sends light to both arms and recombines light coming back. The light not used in detection is reflected onto a recycling mirror that to be sent back to the interferometer. In this way it is foreseen to increase the circulating intensity of light by a factor of about 50, the exact value depending on the losses in the apparatus. The signal is filtered by an output mode cleaner to reduce the contributions from diffuse light and spatial modes that have built up in the interferometer and the intensity is measured by an array of photodiodes. The mirrors, an injection bench supporting the reference cavity and a detection bench with the output mode cleaner are suspended in vacuum to be isolated from seismic and acoustic noise.

7.1. Shot noise

Calculations show that optimal sensitivity is achieved by tuning the interferometer on a "dark fringe", that is with no light going to the photodiodes. In these conditions the phase noise due to photon counting is

$$\tilde{\phi} = \sqrt{\frac{2h\nu}{P\eta}} \tag{16}$$

where P is the light power on the beam splitter, ν is the light frequency, h is the Planck constant and η the photodiode quantum efficiency (negative and positive frequency contributions are summed quadratically.) This translates into an apparent position noise

$$\tilde{x} = \frac{c}{2\pi\nu}\sqrt{\frac{2h\nu}{P\eta}} \tag{17}$$

independent of frequency.

The use of Fabry-Pérot cavities with a finesse $\mathcal{F} = 50$ allows to increase the sensitivity in position by a factor $2\mathcal{F}/\pi \simeq 31.8$. However, according to equation 4, sensitivity will decrease at high frequency.

The resulting photon noise expressed in $\tilde{h}$ is

$$\tilde{h}(\nu_G) = \frac{c}{8L\mathcal{F}\nu}\sqrt{\frac{2h\nu}{P\eta}}\frac{1}{\sqrt{1+(\nu_G/500\,\mathrm{Hz})^2}}. \tag{18}$$

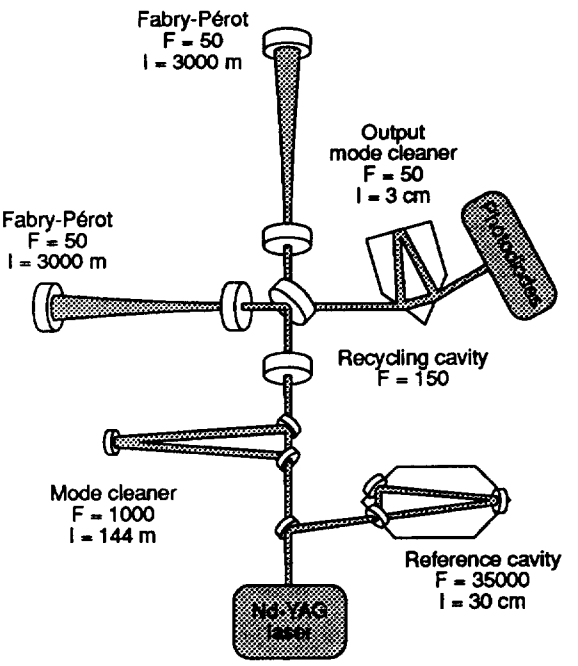

Figure 3. Virgo optical scheme. F is the finesse for the optical cavities. For the recycling cavity this corresponds to a recycling factor of 50. The output mode cleaner is made of fused silica.

7.2. Interferometer control

Maintaining an optimal working point of the interferometer is essential to achieve the best sensitivity. Continuous error measurements are performed and several feedback loops are present in the system to apply the necessary corrections. Laser frequency and intensity stabilization is performed by the Laser Optics group of Orsay as well as the tuning on resonance of the mode cleaner. Similar operations have been studied by LAPP for the output mode cleaner. How to maintain the interferometer on the dark fringe, arm and recycling cavities on resonance involves the whole collaboration: detection of error signals is achieved by measuring the intensity of several beams and mirror position is corrected by acting on the suspensions. A significant effort of dynamic simulation is going on to model the interferometer be-

Table 1
Progress in coatings. Absorption, diffusion and wavefront deformation are given for coatings made in the last years. Measurements are made at 633 and 1064 nm (Virgo working wavelength).

Year	λ nm	Absorb. ppm	Diff. ppm	Wave front λ/n	ϕ_{coat} mm
1992	633	20	50	n/a	25
1994	633	10	5	n/a	50
	1064	2-3	1-2	n/a	50
1995	633	< 0.5	1.2	30	80
	1064	0.5	0.6	n/a	80
Virgo	1064	1	1	100	280

haviour and to design the feedback loops.

Alignment of the interferometer is achieved first by local observation by means of CCD cameras and then by extracting position and angle error signals from the main beams[12]. Computation and experimentation has been performed by LNF on a table-top setup, showing that the method can be applied to a large interferometer.

7.3. Mirror coating and metrology

Performance of the Virgo optical components is crucial to achieve the required sensitivity. A recycling factor of 50 can be achieved only if mirror losses are kept below tens of ppm. Other requirements come from the symmetry between the two arms. Simulations show that 10 ppm absorption in a Fabry-Pérot cavity gives a loss of 3 % on signal; however a 1 ppm asymmetry in absorptions leads to a 40% signal loss[14].

Coating is performed by making use of Dual Ion Beam Sputtering. A coater is being built by IPNL to deal with the large Virgo mirrors. Table 1 shows the results obtained in the last years and how this compares with Virgo specifications that are planned to be met for the final interferometer.

These performances are achieved by successive local corrections of the mirror coating. Several instruments have been set up by ESPCI to achieve the required precision on mirror metrology. If necessary mirror quality could be improved by working on this aspect, which presently sets the limit on the correction process.

8. Vacuum system

The entire interferometer must be enclosed in a vacuum chamber with low residual pressure. Fluctuations in pressure reflect in the index of refraction and so in the actual speed of light. In addition optics need to be protected from pollutants that could worsen performance in the long term.

The main element is the vacuum tube, with diameter 1.2 m. It is equipped with Ti sublimation pumps to achieve a residual pressure of 10^{-9} mbar for H_2. Baffles are placed inside to reduce the amount of diffuse light, which could otherwise reenter the beam and introduce an important phase noise, being modulated by tube wall vibrations.

Towers enclosing the mirror suspensions consist of two vacuum volumes. The upper part containing the seismic filters has a residual pressure of 10^{-6} mbar and the lower part where the marionetta and mirror stay is at 10^{-8} mbar. The marionetta suspension wire passes through a 1 cm diameter conductance pipe connecting the two volumes.

The tube will be constructed and installed under the supervision of Pisa and Orsay, while LAPP follows the construction of the towers.

9. Data acquisition and archiving

When Virgo will be in continuous operation large amounts of data (0.5–1 Mbyte/s) will have to be recorded for off line analysis. Design of the data acquisition and recording system is being done by LAPP, while Napoli is designing the archiving system for the data produced, including environment monitoring. The acquisition system features an online fast selection of data that could possibly contain coalescences or collapses.

10. Design sensitivity

The expected Virgo performance can be summarized by a sensitivity curve giving the spectral amplitude of a gravitational wave such that

SNR = 1 in each 1 Hz frequency bin. Figure 4 shows the sensitivity together with the most important noise contributions.

Improvements can come from developments on thermal noise of the suspension wires and of the mirrors. This will require experimentation to optimize wire clamp design and on new materials and fabrication processes to improve the current figures of merit. Sensitivity increase at high frequency is expected with the development of higher power lasers.

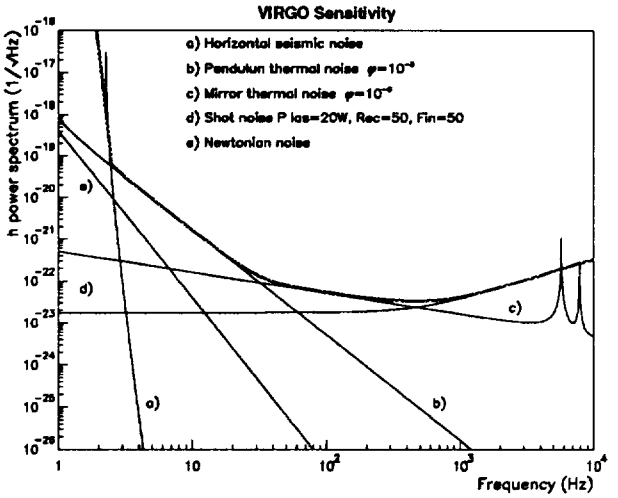

Figure 4. The VIRGO design sensitivity (SNR=1) and the main contributions to noise.

11. Schedule and perspectives

Ground work has started in May 1996 after Virgo was given permission to occupy the necessary land on site. The construction plan foresees the completion of the central area buildings by mid '97. An important step will be the commissioning in '98 of a Michelson interferometer situated in the central building that makes use of the final suspension system. This interferometer will be used to debug and test all the equipment of the central area: laser, and injection bench, mode cleaner, detection bench, suspensions and the related control electronics and software. This learning period should provide measurements of several noise terms with adequate sensitivity, allowing for improvements and corrections.

In the mean time arm construction will start together with vacuum tube installation and light is expected to circulate in the full interferometer by mid 2000.

REFERENCES

1. F.W.Dyson, A.S.Eddington and C.Davidson, Phil. Trans. Roy. Soc. **220A** (1920) 291.
2. C.M.Will, *"Theory and experiments in gravitational physics"*, Cambridge University Press, Cambridge, UK, 1993.
3. R.V.Pound and G.A.Rebka, Phys. Rev. Lett. **4** (1960) 337.
4. C.W.Misner, K.S.Thorne and J.A.Wheeler, *Gravitation*, Freeman, S.Francisco, 1973.
5. Hulse R.A. and J.H.Taylor, Ap. J. **195** (1975) L51.
6. J.H.Taylor *et al* , Nature **355** (1992) 132.
7. K.S.Thorne, *"Gravitational Radiation"*, in *300 Years of Gravitation*, S.W.Hawking and W.Israel eds., Cambridge, 1987, p. 362.
8. G.Veneziano, *"3rd Colloque Cosmologie"*, Paris, June 1995, preprint CERN-TH/95-254.
9. J.H.Taylor, R.N.Manchester and A.G.Lyne, Ap. J. Suppl. **88** (1993) 529.
10. H.B.Callen and R.F.Greene, Phys. Rev. **86** (1952) 702.
11. P.R.Saulson, Phys. Rev. **D42** (1990) 2437.
12. N.M.Sampas and D.Z.Anderson, Appl. Opt **23** (1990) 394. and references therein
13. ULE is a trademark of Corning Inc., New York, USA.
14. C.Boccara *et al* , Proceedings of *"Int. Conf. on Gravitational Waves: Sources and Detectors"*, I.Ciufolini and F.Fidecaro eds., to be published by WSP, Singapore.